batteries

MDPI

Supplementary Information

Nickel-Doped Ceria Bifunctional Electrocatalysts for Oxygen Reduction and Evolution in Alkaline Media

Jadranka Milikić [1], Rodolfo O. Fuentes [2], Julia E. Tasca [3], Diogo M. F. Santos [4,*], Biljana Šljukić [1,4] and Filipe M. L. Figueiredo [5,*]

[1] University of Belgrade, Faculty of Physical Chemistry, Studentski trg 12–16, 11158 Belgrade, Serbia; jadranka@ffh.bg.ac.rs (J.M.); biljka@ffh.bg.ac.rs (B.Š.)
[2] Instituto de Nanociencia y Nanotecnología, Departamento de Física, Centro Atómico Constituyentes, CNEA-CONICET, Av. Gral. Paz 1499, San Martín, Buenos Aires B1650, Argentina; rofuentes@conicet.gov.ar
[3] CIFICEN (UNCPBA-CICPBA-CONICET), Facultad de Ingeniería–UNCPBA, Av. Del Valle 5737, Olavarría B74001WI, Argentina; jtasca@fio.unicen.edu.ar
[4] Center of Physics and Engineering of Advanced Materials (CeFEMA), Laboratory for Physics of Materials and Emerging Technologies (LaPMET), Chemical Engineering Department, Instituto Superior Técnico, Universidade de Lisboa, 1049–001 Lisbon, Portugal
[5] CICECO, Physics Dept., University of Aveiro, Campus Universitário de Santiago, 3810-193 Aveiro, Portugal
* Correspondence: diogosantos@tecnico.ulisboa.pt (D.M.F.S.); lebre@ua.pt (F.M.L.F.)

Citation: Milikić, J.; Fuentes, R.O.; Tasca, J.E.; Santos, D.M.F.; Šljukić, B.; Figueiredo, F.M.L. Nickel-Doped Ceria Bifunctional Electrocatalysts for Oxygen Reduction and Evolution in Alkaline Media. *Batteries* **2022**, *8*, 100. https://doi.org/10.3390/batteries8080100

Academic Editor: Seung-Tae Hong

Received: 24 July 2022
Accepted: 17 August 2022
Published: 19 August 2022

Publisher's Note: MDPI stays neutral with regard to jurisdictional claims in published maps and institutional affiliations.

Supplementary Information

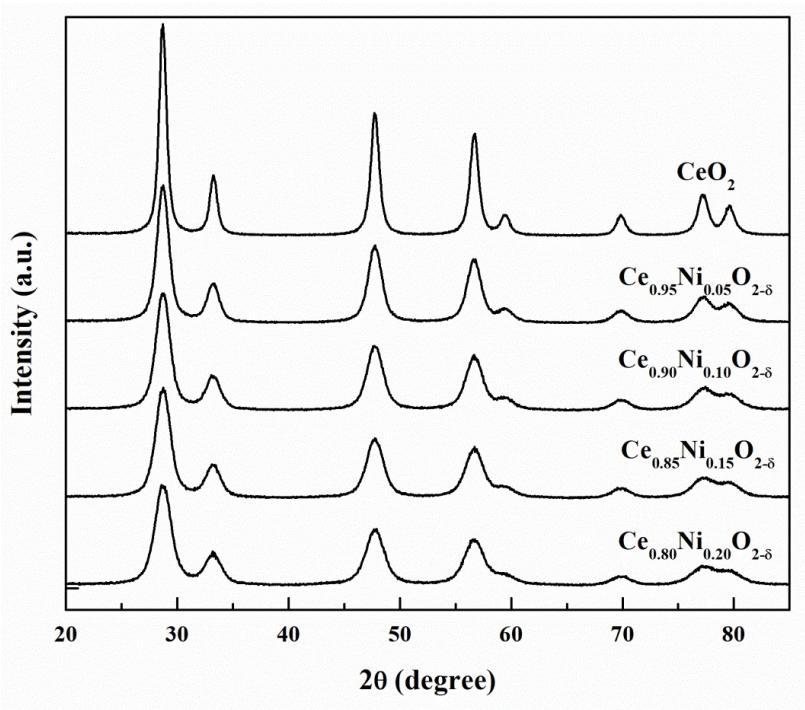

Figure S1. Synchrotron radiation powder X-ray diffraction (SR-XRD) patterns recorded at room temperature for the nanostructured $Ce_{1-x}Ni_xO_{2-\delta}$ materials.

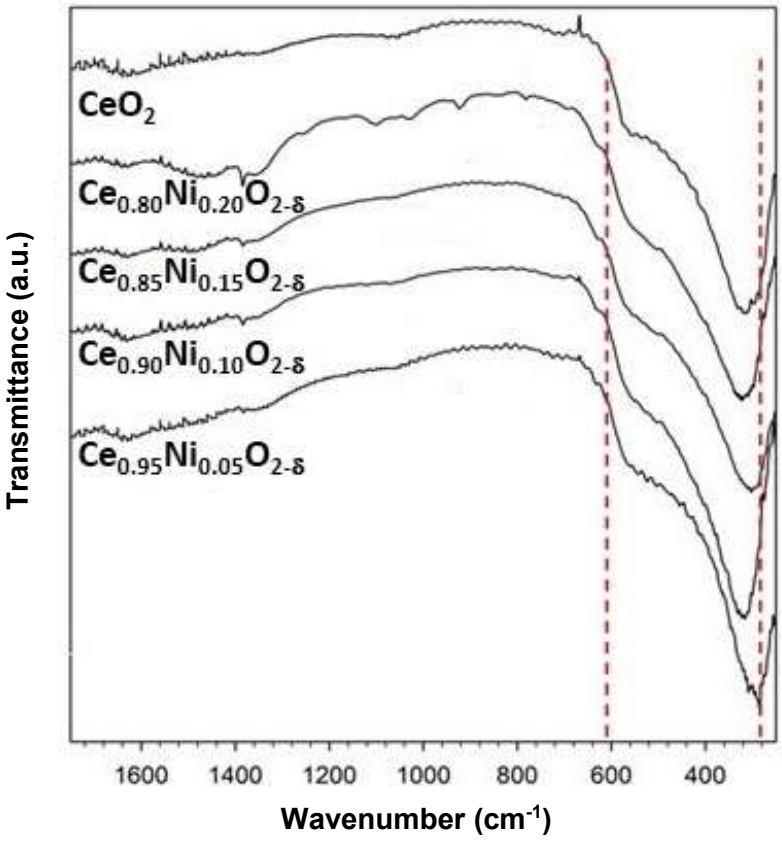

Figure S2. Fourier transform infrared spectra (FTIR) spectra of the $Ce_{1-x}Ni_xO_{2-\delta}$ nanopowders.

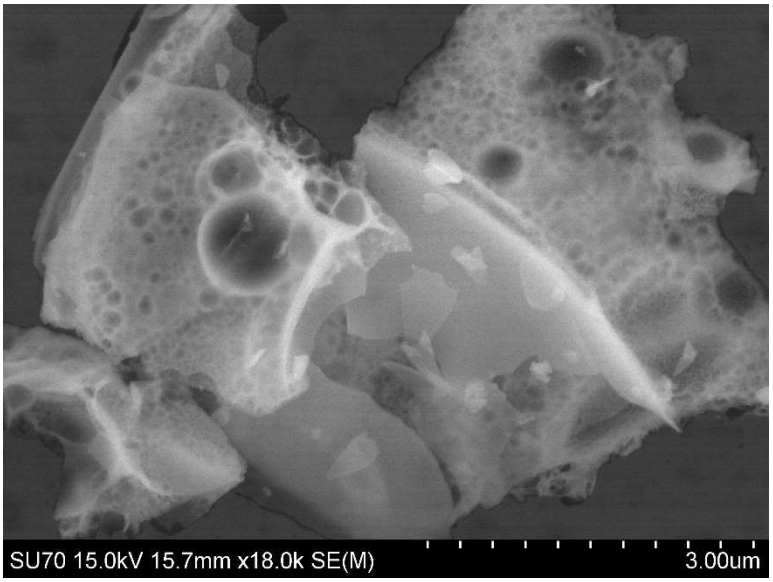

Figure S3. Low-resolution scanning transmission electron microscopy (STEM) image of the $Ce_{0.90}Ni_{0.10}O_{2-\delta}$ sample obtained on a Scanning Electron Microscope equipped with a transmission detector (Hitachi SU 70).

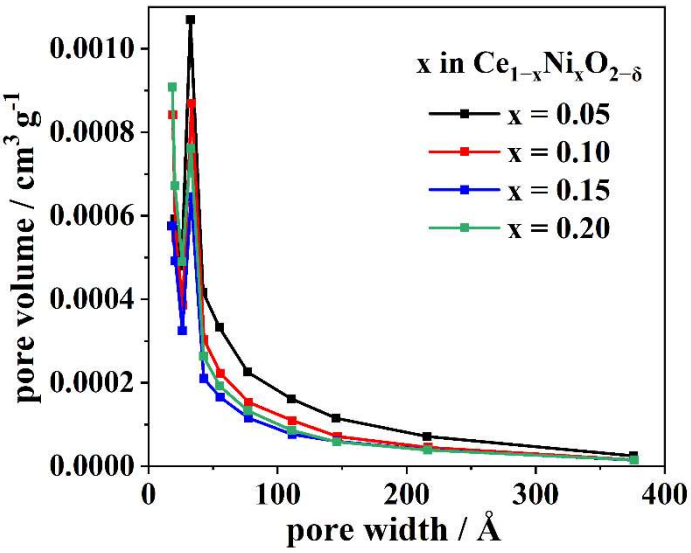

Figure S4. Pore size distribution for the $Ce_{1-x}Ni_xO_{2-\delta}$ nanopowders estimated from the nitrogen desorption data using the Barrett-Joyner-Halenda method utilizing the Halsey thickness curve with the G.S. Faass correction.

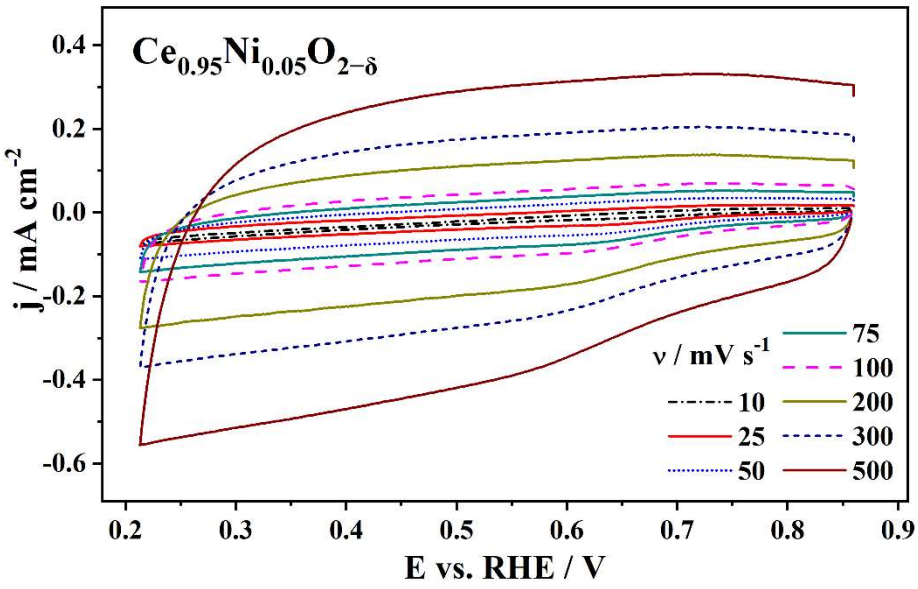

Figure S5. Cyclic voltammograms of $Ce_{0.95}Ni_{0.05}O_{2-\delta}$ in deaerated 0.1 M KOH electrolyte solution at scan rates ranging from 10 to 500 mV s^{-1}.

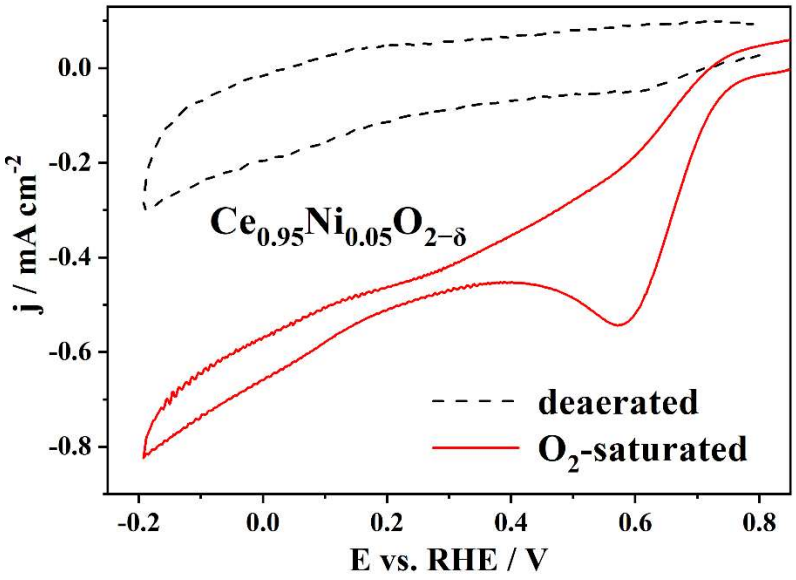

Figure S6. Voltammetric response of $Ce_{0.95}Ni_{0.05}O_{2-\delta}$ in deaerated and O_2-saturated 0.1 M KOH.